A&A 400, 939–950 (2003)
DOI: 10.1051/0004-6361:20030135

Astronomy & Astrophysics

Spectral analysis of sdB stars from the Hamburg Quasar Survey⋆,⋆⋆

H. Edelmann[1], U. Heber[1], H.-J. Hagen[2], M. Lemke[1], S. Dreizler[3], R. Napiwotzki[1], and D. Engels[2]

[1] Dr. Remeis-Sternwarte, Astronomisches Institut der Universität Erlangen-Nürnberg, Sternwartstr. 7, 96049 Bamberg, Germany
[2] Hamburger Sternwarte, Gojenbergsweg 112, 21029 Hamburg, Germany
[3] Institut für Astronomie und Astrophysik, Sand 1, 72076 Tübingen, Germany

Received 3 May 2002 / Accepted 17 January 2003

Abstract. We present the results of a spectral analysis of a large sample of subdwarf B stars selected from follow-up observations of candidates from the Hamburg Quasar Survey. Fundamental parameters (effective temperature, gravity, and helium abundance) were determined by matching synthetic line profiles calculated from model atmospheres to all hydrogen and helium absorption lines present in the observed optical spectra. The derived helium abundances are compared with the atmospheric parameters to search for possible trends. We discovered a correlation between the helium abundance and the effective temperature: the larger the temperature, the larger the photospheric helium content of sdB stars. Additionally, a separation into two sequences of sdB stars in the effective temperature – helium abundance plane is detected. We compared our analysis results with data from the literature. The stars from our sample are found to be somewhat more luminous. This can only partly be explained by NLTE effects. Three apparently normal B stars were discovered, which could be massive stars far away from the galactic plane (7–19 kpc). Radial velocities were measured for 23 stars from which we discovered a new radial velocity variable sdB star.

Key words. stars: abundances – stars: atmospheres – stars: distances – stars: horizontal-branch – stars: subdwarfs

1. Introduction

The Hamburg Quasar Survey (HQS) was carried out, starting in 1980, with the 80 cm Schmidt telescope at the German-Spanish Astronomical Center (DSAZ) on Calar Alto, Spain (Hagen et al. 1995). Although it was primarily initiated as a quasar survey, it is also a very rich source of faint blue stars. Unlike the Palomar Green (PG) survey (Green et al. 1986) and most other surveys, objective prism spectra (spectral resolution of 45 Å FWHM at H_γ) were obtained. Afterwards, the HQS plates were digitized in Hamburg using a PDS microdensitometer. A search software selects quasar candidates as well as faint blue stars from the 30 000–50 000 spectra per plate in the magnitude range of $13\overset{m}{.}5 \leq B \leq 18\overset{m}{.}5$. Selection criteria are blue continua and/or emission lines (Hagen et al. 1995).

In a collaboration between the institutes in Hamburg, Kiel, Tübingen, and Bamberg, follow-up observations and analyses of visually selected candidates of hot stars were performed.

The current database of follow-up observations contains well over 400 confirmed stars. The dominant fractions of the list are hot subdwarfs (∼50%) and white dwarfs (∼30%). A lot of very rare and unusual stars also were found. The discovery of four PG 1159, nine hot DO, and five DAO white dwarfs, so far, are the highlights of the follow-up observations (Heber et al. 1996 and references therein). A comprehensive summary of the results from the HQS follow-up observations of hot stars can be found in Heber et al. (1991), Dreizler et al. (1994), Lemke et al. (1997a, sdO stars), and Homeier et al. (1998, 1999, DA white dwarfs).

The present analysis focuses on the subluminous B, or *subdwarf* B (sdB) stars discovered by our campaigns of follow-up spectroscopy. In the Hertzsprung-Russell-Diagram (HRD), sdB stars populate a very narrow area which lies on a blueward extension of the horizontal branch (HB), the so called *extreme horizontal branch* (EHB, Heber et al. 1984; Heber 1986; Saffer et al. 1994). They have hydrogen dominated atmospheres (typically: $n(\mathrm{He})/n(\mathrm{H}) \lesssim 0.01$), with effective temperatures of $20\,000\mathrm{K} \leq T_{\mathrm{eff}} \leq 40\,000\mathrm{K}$ and their logarithmic surface gravities are typically between 5.0 and 6.0 (cgs). SdB stars consist of a helium-burning core with a canonical mass of $M_{\mathrm{core}} \approx 0.5\ M_\odot$

Send offprint requests to: H. Edelmann,
e-mail: edelmann@sternwarte.uni-erlangen.de

⋆ Based on Observations collected at the German-Spanish Astronomical Center (DSAZ), Calar Alto, operated by the Max-Planck-Institut für Astronomie Heidelberg jointly with the Spanish National Commission for Astronomy.

⋆⋆ Table 4 is only available in electronic form at the CDS via anonymous ftp to cdsarc.u-strasbg.fr (130.79.128.5) or via http://cdsweb.u-strasbg.fr/cgi-bin/qcat?J/A+A/400/939

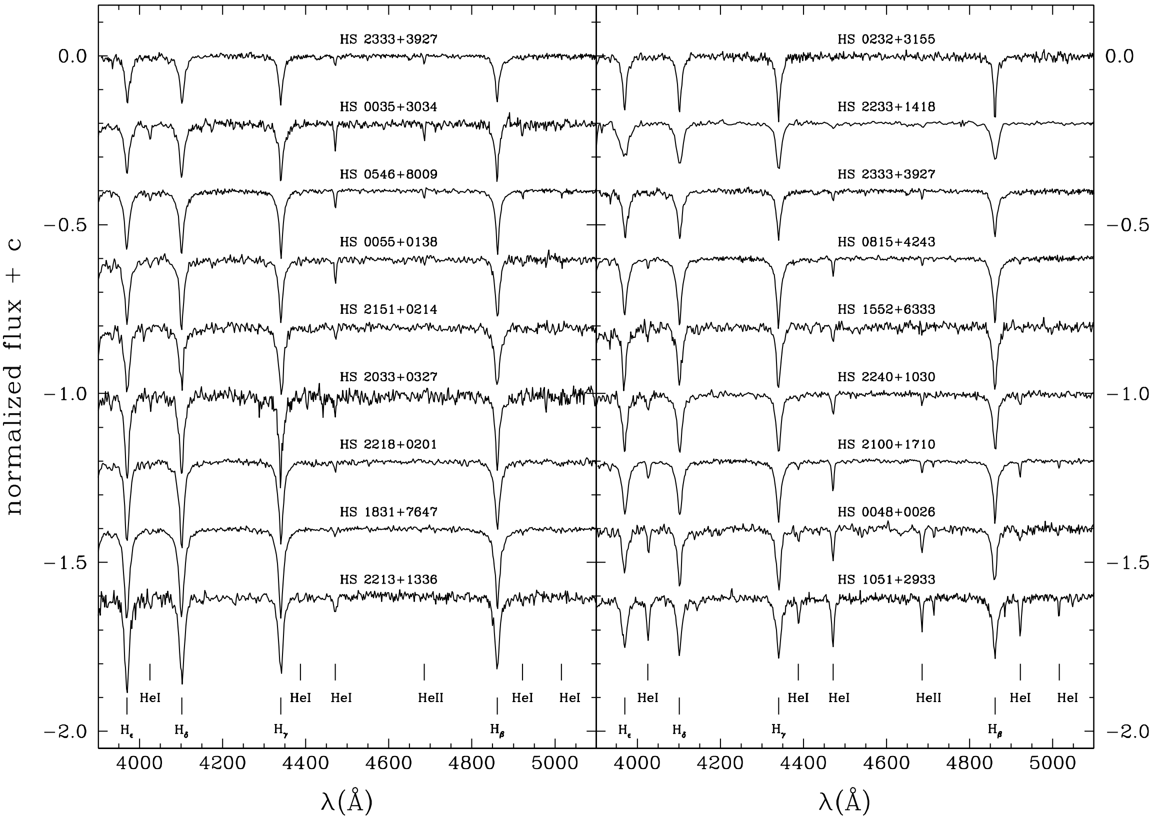

Fig. 1. Normalized spectra of selected programme stars. Left hand panel: The spectra are arranged in order of effective temperature, ranging from ~20 000 K at the bottom to ~38 500 K at the top. The selected stars all have roughly similar gravities and helium abundances ($\log(g) \approx 5.5$ [cgs], $n(\mathrm{He})/n(\mathrm{H}) \approx 0.01$). Right hand panel: Helium abundance variations: $n(\mathrm{He})/n(\mathrm{H}) < 10^{-4}$ at the top to $n(\mathrm{He})/n(\mathrm{H}) \sim 0.25$ at the bottom. The selected stars all have roughly similar effective temperatures and gravities ($T_{\mathrm{eff}} \approx 35\,000$ K, $\log(g) \approx 6.0$ [cgs]).

surrounded by a thin hydrogen-rich envelope ($M_{\mathrm{env}} < 0.02\,M_{\odot}$, Heber 1986; Saffer et al. 1994). However, their origin is still unclear.

After passing the red-giant stage, these stars must have suffered from such a high mass loss rate that their outer layer was lost almost entirely. The remaining hydrogen-rich envelope has not enough mass to sustain a hydrogen-burning shell. This means that the star cannot ascend the asymptotic giant branch (AGB) after the end of the helium-core burning, but should evolve like a 0.5 $M_{\odot}$ helium-main-sequence star (Heber et al. 1984; Heber 1986). Calculations of Dorman et al. (1993) support this idea. The reason for very high mass loss at or shortly after the core helium flash is still unclear and several scenarios are discussed. As to the origin of sdB stars, a plausible hypothesis is close binary evolution (Mengel et al. 1976). In addition to the composite spectrum binaries (Allard et al. 1994; Theissen et al. 1993, 1995 and others) several single-lined binary sdB stars have been identified from variable Doppler line; Maxted et al. 2001; Green et al. 2001). At least two thirds of local disk sdB stars are found to be binaries.

SdB stars are important to understand galaxy evolution. They are the main cause for the UV excess, the so-called *UV upturn*, in elliptical galaxies and galaxy bulges (Brown et al. 1997; Brown et al. 2000b). The reason is that sdB stars spend a long life time ($\sim 10^8$ years) on the EHB at high temperatures. They are also considered to be useful age indicators for elliptical galaxies (Brown et al. 2000a). Subdwarf B stars are also very important in the context of stellar astrophysics. The discovery of several pulsating sdB stars (called sdBV or EC 14026 stars, after the prototype EC 14026−2647, Kilkenny et al. 1997) has rapidly increased the interest in these objects, because of the prospect of probing their structure by asteroseismology. The driving mechanism of the pulsation is due to an opacity bump associated with an iron ionization in the envelopes of sdB stars (Charpinet et al. 1996, 1997). The prediction of Charpinet et al. (1997) that sdB stars in the temperature range of $29\,000\mathrm{K} \leq T_{\mathrm{eff}} \leq 36\,000$ K should pulsate is very well confirmed by subsequent spectroscopical analyses of the EC 14026 stars (Heber et al. 2000; Østensen et al. 2000a, b, Dreizler et al. 2002; Silvotti et al. 2002). Now, 29 pulsating sdB stars are known (see O'Donoghue et al. 1999; Charpinet 2001 for reviews).

For all these investigations, knowledge of the stellar parameters is very important. We present here the results of a spectral analysis of a large sample of subdwarf B stars selected from follow-up observations of candidates from the Hamburg Quasar Survey.

2. Programme stars

2.1. Preselection

Candidate stars were selected from the HQS objective prism plates, first by automatically selecting spectra which are blue

Table 1. Observing logs of all HQS follow-up runs for our programme stars. A range of spectral resolutions is given for the three runs affected by seeing disk being temporarily smaller than the slit width.

run #	date (start of nights)	instrument	recip. disp. [Å/mm]	spectr. res. [Å]	wavelength coverage [Å]	observers
1	1989 Jan. 21–25	3.5 m B&C	120	5.0	3850–5650	Heber & Jordan
2	1990 Jan. 08–17	3.5 m TWIN	144/160	6.5	3550–5550, 5570–7030	Jordan & Möller
3	1990 Oct. 01–09	3.5 m FR	136	7.0	3770–5550	Heber & Dreizler
4	1990 Nov. 04–11	3.5 m TWIN	144/160	5.5	3430–5550, 5560–7030	Jordan & Rauch
5	1991 Jun. 19–25	3.5 m TWIN	144/160	5.5	3570–5750, 5110–9300	Heber & Marten
6	1992 Sep. 10–14	3.5 m TWIN	144/160	4.5-5.5	3360–5550, 5430–9740	Dreizler
7	1993 Mar. 07–12	3.5 m TWIN	144/160	5.0	3470–5680, 5420–9630	Heber
8	1993 Aug. 28–Sep. 02	3.5 m TWIN	72/72	3.4	3600–5500, 5540–7420	Dreizler & Haas
9	1993 Sep. 02–05	2.2 m CAS	120	4.5-5.5	4010–6720	Haas & Dreizler
10	1994 Sep. 21–25	3.5 m TWIN	72/72	3.5	3610–5490, 5440–7320	Dreizler
11	1995 Jan. 23–27	3.5 m TWIN	72/72	3.5	3580–5470, 5420–7320	Dreizler
12	1996 Aug. 16–19	3.5 m TWIN	72/72	3.6	3770–5660, 5430–7340	Lemke
13	1997 Aug. 28–31	3.5 m TWIN	72/72	3.5	3300–5450, 5300–7550	Edelmann
14	1998 Sep. 30–Oct. 04	2.2 m CAFOS	100	5.0-8.0	3400–6300	Edelmann

compared to the bulk of spectra, and second, by visually classifying them on a graphics display (Hagen et al. 1999). Objects with UV excess emission were either classified directly as hot stars due to the presence of hydrogen Balmer absorption lines or were retained as quasar candidates. Follow-up observations of stellar candidates were mostly made from the hot stars list, and occasionally were of objects that were not confirmed as quasars.

2.2. Observations

The observations described here were obtained, starting in January 1989, at the DSAZ on Calar Alto, Spain, during various observing runs with different telescopes and instruments. The observational dataset is therefore very inhomogeneous. The spectral resolution ranges from 3.4 Å to 8.0 Å FWHM (determined from the FWHM of the helium-argon lines in the calibration spectra) and the wavelength coverage also varies between 4010–6720 Å and 3360–9740 Å. For three observing runs the seeing was sometimes better (smaller) than the slit width, resulting additionally in a varying spectral resolution during these runs. For a detailed overview of the observational material see Table 1.

2.3. Data reduction

The spectra were extracted from the two-dimensional frames and reduced to linear wavelength and intensity scales using the IDAS package written by G. Jonas in Kiel for the early observations (until 1991) and the ESO-MIDAS package for the data obtained after 1991.

All frames were bias subtracted, flat field corrected, and cosmic ray events were cleaned. The sky background was removed by extracting a stripe on each side of the star's spectrum and subtracting the average of these two stripes from each row of the stellar signal on the CCD. These corrected rows were combined to a one dimensional stellar spectrum. Thereafter a wavelength calibration was performed with calibration spectra recorded immediately after each stellar spectrum. Then all wavelength-calibrated spectra were corrected for atmospheric extinction using the extinction coefficients of La Silla, Chile (Tüg 1977) as these coefficients are not available for the Calar Alto observatory. In the last step all spectra were relatively flux calibrated using spectra of flux-standard stars (mostly BD+28° 4211, G 191−B2B or Feige 34, Oke 1990) which were taken each night.

A subset of spectra obtained is presented in Fig. 1. The object list is supplemented by one spectrum of a sdB star (HS 1641+4601) kindly provided by T. Rauch.

2.4. Selection and classification

From the list of stellar HQS follow-up observations, we selected here 111 subdwarf B candidates for a detailed analysis, using the classification system of Moehler et al. (1990b): The optical spectra of subdwarf B stars are dominated by strong broad Balmer lines of neutral hydrogen and weak or absent He I lines. The so-called sdOB stars, introduced by Baschek & Norris (1975), represent a hotter group of the sdB stars, that show in addition to strong broad Balmer and weak He I lines a weak He II 4686 Å absorption line in their spectra.

A closer inspection revealed 18 sdB stars of the sample to be spectroscopic binaries. All of them show at least two characteristics of a cool companion star (e.g. flat flux distribution, G-band absorption, Ca H+K, Mg I triplet at 5167 Å, 5173 Å, and 5184 Å) (see Table 2). The spectral classifications for all programme stars are listed in Table 4.

The coordinates were determined on HQS direct plates and are accurate to ±2″. We checked the Digital Sky Survey for all stars and found that usually the object cannot be mistaken. Stars nearby were found in eight cases and for those we present finding charts in Fig. 9. The B-magnitudes presented in Table 4 were determined mostly from the objective prism plates and may have an error of up to 0.3 mag except when marked by a colon (±0.5 mag uncertainty).

Table 2. Spectral signatures of cool companion stars in the spectroscopic binaries of our sample.

binary stars	Ca H+K	*G*-band	Mg I	flat flux
HS 0028+4407	√	√	√	√
HS 0127+3146	–	√	√	–
HS 0136+0605	–	–	√	√
HS 0215+0852	–	√	√	√
HS 0252+1025	–	√	√	√
HS 0446+1344	–	√	√	√
HS 0656+6117	–	√	√	–
HS 0942+4608	√	√	√	√
HS 1106+6051	√	√	√	√
HS 1511+6221	√	√	√	–
HS 1612+6337	√	√	√	√
HS 1612+7335	√	√	√	√
HS 1615+6341	–	√	√	√
HS 1753+5342	√	√	√	√
HS 1753+7025	√	√	√	√
HS 1844+5048	–	√	√	–
HS 1858+5736	√	–	√	√
HS 2216+1833	√	√	√	√

Several stars have already been discovered as UV excess objects independently by various surveys. The references are indicated in Table 4. Although 45 of our programme stars can be found in other surveys, we found spectral classifications for only 21 of them in the literature. As can be seen in Table 3 there is a good agreement with previous classifications except for HS 2333+3927 which was previously classified as a DAZ white dwarf.

3. Atmospheric parameters

The stellar atmospheric parameters (effective temperature, surface gravity, and photospheric helium abundance) were determined by matching synthetic line profiles calculated from model atmospheres to all Balmer (mainly H_β up to H_ϵ) and helium (mainly He I $\lambda\lambda$ 4026 Å, 4471 Å, 5015 Å, 5876 Å, and He II 4686 Å) line profiles present in the observed spectra of all programme stars.

3.1. Model atmospheres and synthetic spectra

Three different sets of models were used:

1. A grid of metal-line blanketed LTE model atmospheres (Heber et al. 2000). The models are plane parallel and chemically homogeneous and consist of hydrogen, helium, and metals (solar abundances). The synthetic spectra were calculated with LINFOR[1].

[1] LINFOR was originally developed by H. Holweger, M. Steffen, and W. Steenbock at Kiel University. It has been enhanced and maintained by M. Lemke, with additional modifications by N. Przybilla. For a description see:
`http://www.sternwarte.uni-erlangen.de/~ai26/linfit/linfor.html`

Table 3. Comparison of spectral classifications with previous work. Since the PG classification scheme differs from ours, we transcribed the PG spectral types into our scheme (Moehler et al. 1990b).

star	this work	other	Ref. & name within
HS 0016+0044	sdB	sdB	T94
HS 0039+4302	sdB	sdB	B91: Balloon 84041013
HS 0048+0026	sdOB	sdB	B91: Balloon 94700002
		sdOB	G86: PG 0048+004
HS 0055+0138	sdB	sdB	B91: Balloon 94700001
		sdB	P86: PG 0055+016
HS 0209+0141	sdB	sdB	G86: PG 0209+0141
HS 0212+1446	sdB	sdB	G86: PG 0212+148
HS 0232+3155	sdOB	sdB	W90: KUV 02324+3156
HS 0941+4649	sdB	sdB	M98: US 909
HS 0942+4608	binary	sdB+G	H89
		sdB	M98: PG 0942+461
HS 1106+6051	binary	sdB	G86: PG 1106+608
HS 1236+4745	sdB	sdB	S94: PG 1236+479
HS 1511+6221	binary	sdB+K5	A94: PG 1511+624
		sdB	A96: FBS 1511+624
HS 1547+6312	sdB	sdB	A96: FBS 1547+632
		sdB	G84: PG 1547+632
HS 1612+7335	binary	sdB+K2.5	A94: PG 1612+735
HS 1641+4601	sdB	sdB	B91: Balloon 83600002
HS 2218+0201	sdB	sdB	U98: PG 2218+020
HS 2233+2332	sdOB	sdB	B91: Balloon 90900003
HS 2240+0136	sdB	sdOB?	K84: PHL 384
HS 2240+1031	sdOB	sdB	G84: PG 2240+105
HS 2246+0158	sdB	sdB	G84: PG 2246+019
HS 2333+3927	sdOB	DAZ	A96: FBS 2333+395

Ref.: A94 = Allard et al. (1994); A96 = Abrahamian & Mickaelian (1996); B91 = Bixler et al. (1991); G86 = Green et al. (1986); H89 = Heber et al. (1989); K84 = Kilkenny (1984); M98 = Mitchell (1998); R93 = Rodgers et al. (1993); S94 = Saffer et al. (1994); T94 = Thejll et al. (1994); W90 = Wegner et al. (1990).

For the spectrum synthesis, line profiles were calculated for the Balmer series of neutral hydrogen (n up to 22) with Stark broadening tables of Lemke (1997b) which uses the unified theory of Vidal et al. (1973). Helium lines were calculated using broadening tables of Barnard et al. (1974), Shamey (1969), and Griem (1974) for He I, and Schöning & Butler (1989) for He II. The metal line blanketing was included by the opacity distribution function (ATLAS6) of Kurucz (1979). The grid covers the area for EHB Stars: $T_{\rm eff}$ = 11 000 K ... 35 000 K in steps of $\Delta T_{\rm eff}$ = 1000 K to 2500 K; $\log(g)$ = 3.50 ... 6.50 [cgs] in steps of $\Delta\log(g)$ = 0.25; $n({\rm He})/n({\rm H})$ = 0.0001, 0.001, 0.01, 0.03, 0.10, 0.33.

2. A grid of partially line blanketed NLTE model atmospheres (Napiwotzki 1997). The models are plane parallel, chemically homogeneous, and consist of hydrogen and helium. The latest version of the NLTE code from Werner (1986) was used which is based on the Accelareted Lambda Iteration (ALI) of Werner & Husfeld (1985). The following grid was used: $T_{\rm eff}$ = (27, 30, 32, 35, 37, 40, 45) × 1000 K; $\log(g)$ = 3.50 ... 6.50

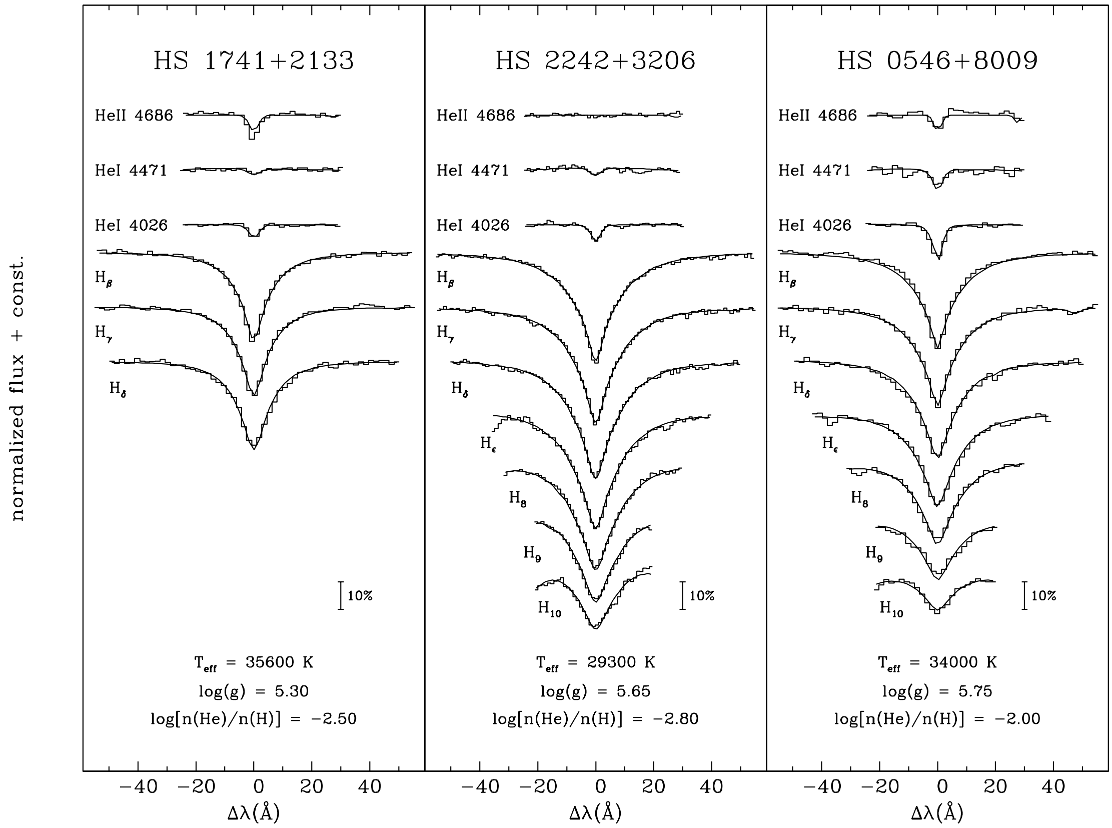

Fig. 2. Sample fits for three programme sdB stars. The observed spectra are plotted as histograms. A detailed discussion of the fit for HS 1741+213 is given in Sect. 3.2.

in steps of $\Delta \log(g) = 0.25$; $n(\mathrm{He})/n(\mathrm{H}) = 3 \times 10^{-4}, 1 \times 10^{-3}, 3 \times 10^{-3}, 0.01, 0.03, 0.1, 0.3$.

3. A grid of partially line blanketed NLTE model atmospheres for He-rich ($n(\mathrm{He})/n(\mathrm{H}) > 0.3$) objects. An extended and updated grid of Dreizler et al. (1990), based on the ALI method, was used. The models are plane parallel and chemically homogeneous and consist of hydrogen and helium. The grid covers: $T_{\mathrm{eff}} = (35, 40, 45) \times 1000$ K; $\log(g) = 4.0 \ldots 6.5$ in steps of $\Delta \log(g) = 0.5$; $n(\mathrm{He})/n(\mathrm{H}) = 0.5, 1, 3, 10, 100$.

3.2. Fit procedure

The matching of the observed spectra was done by means of a χ^2 fit using an updated procedure of Bergeron et al. (1992) and Saffer et al. (1994) which determines simultaneously the atmospheric parameters. Beforehand all spectra were normalized and the model spectra were folded with the instrumental profile (Gaussian with appropriate width). Rotational broadening was neglected in the fitting procedure. Some fit examples are shown in Fig. 2.

The numbers of Balmer lines that can be used for the analysis may be limited by insufficient spectral coverage. Hence several stars are left with only three Balmer lines (see Fig. 2). In order to check whether the results depend on the number of Balmer lines included in the fit, we compared results based on many Balmer lines to those from three lines for stars with sufficient spectral coverage. No systematic differences became apparent.

The fit reproduces the Balmer lines well. For the hottest stars the He I/He II ionisation equilibrium provides an additional temperature indicator. In most cases (e.g. HS 0546+8009, see Fig. 2) the fit of the He I and He II lines is consistent with that of the Balmer lines. However, for sdOB stars showing a He II 4686 Å line which is comparable or stronger than the He I 4471 Å line (i.e. for HS 0048+0026, HS 1051+2933, HS 1741+2133, HS 2156+2215, and HS 2333+3927), the helium ionisation equilibrium indicates a considerably higher effective temperature than from the Balmer lines. The most extreme case is HS 1741+2133 displayed in Fig. 2 (left panel). To match the He II line an effective temperatute larger by ≈3000 K would be required. Such a discrepancy has also been observed in the analysis of high resolution spectra of the pulsating sdB star PG 1219+534 (Heber et al. 2000). A detailed discussion is given in that paper. In the absence of an explanation for this helium line problem we adopt the parameters from the fit of all lines (H+He).

Our fit process, however, fails in the case of composite spectra. Without knowledge of the flux distributions of the cool companions it is impossible to extract the spectra of the sdB stars. To analyse these binaries, additional spectra and more sophisticated procedures are necessary (see e.g.

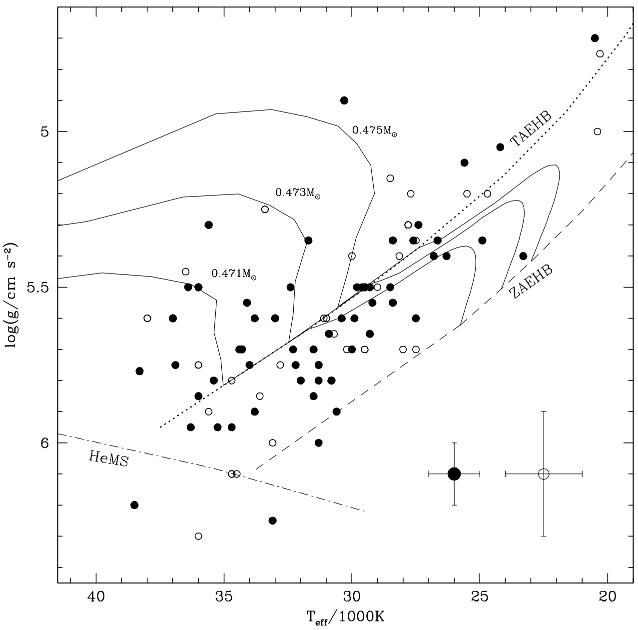

Fig. 3. Distribution of our sdB sample in the $T_{\rm eff}$–log(g)-plane. Stars denoted by open circles have larger uncertainties for the derived temperatures and gravities than the stars denoted by filled circles (see typical error-bars at the lower right side) mostly due to lower S/N and/or spectral resolution. The Helium Main Sequence (HeMS, Paczyński 1972) together with the Zero Age Extended Horizontal Branch for solar metallicity (ZAEHB), the Terminal Age Extended Horizontal Branch for solar metallicity (TAEHB), and evolutionary tracks for extended horizontal branch stars from Dorman et al. (1993) for three different masses (solar metallicity) are shown for comparison.

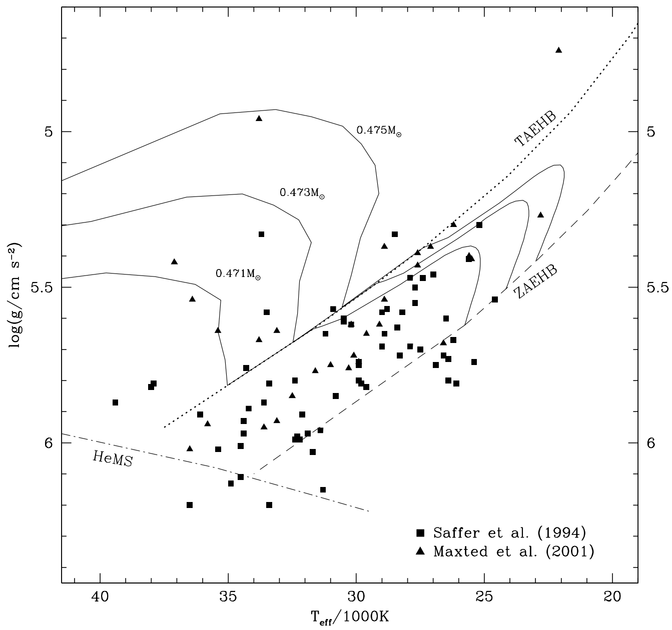

Fig. 4. Distribution of the sdB samples of Saffer et al. (1994, filled squares) and Maxted et al. (2001, filled triangles) in the $T_{\rm eff}$–log(g)-plane for comparison purposes (see Sects. 3.4 and 5).

Aznar Cuadrado & Jeffery 2002). We defer the analysis of the composites to a subsequent paper.

3.3. Results

Table 4 summarizes the results of our analysis including spectral types, effective temperatures, gravities, and helium abundances. Additionally, the equatorial and galactical coordinates, the B magnitudes and extinctions, the radial velocities (see Sect. 4.1), the absolute visual magnitudes, the distances from earth and from the galactic plane (see Sect. 4.2), and the references are given for all programme stars. The values given with 27 000 K $\leq T_{\rm eff} \leq$ 35 000 K represent mean results of our LTE and non-LTE fits. All values with $T_{\rm eff} <$ 27 000 K are exclusively from LTE, and all values with $T_{\rm eff} >$ 35 000 K are solely from non-LTE fits. Statistical errors for the atmospheres which are derived from the fit program are unrealistically small (typically: $\sigma^{\rm fit}_{T_{\rm eff}} \approx$ 300 K, $\sigma^{\rm fit}_{\log(g)} \approx$ 0.05 dex, $\sigma^{\rm fit}_{\log[n({\rm He})/n({\rm H})]} \approx$ 0.05 dex). The systematic errors that arise from the observations (spectral resolution, S/N), and from the data reduction (flat-field correction, background subtraction, relative flux calibration, and continuum placement) are dominant. The real errors can only be estimated. Individual error estimates for the effective temperatures, the gravities, and helium abundances are given in Table 4. Four EHB programme stars which are observed twice at different dates with different instruments allow a selfconsistency check. As can be seen, the results match well within the given error limits. In these cases the mean results are plotted in Fig. 3.

The analysis shows that 89 (~96%) of the 93 selected apparently single stars are bona fide sdB or sdOB stars. One (HS 2229+0910) is considered to be a blue horizontal branch (HBB) star, while three stars (HS 0231+8019, HS 1556+6032, and HS 2131+0349) have atmospheric parameters consistent with those of normal main sequence B stars. One of the sdOB stars (HS 1051+2933) is identified as unusually helium rich, i.e. exceeding the solar helium abundance. The results for all apparently single programme sdB stars are also shown in Fig. 3 in a $T_{\rm eff}$–log(g)-diagram. For comparison we plot the results of the analyses of sdB stars by Saffer et al. (1994) and Maxted et al. (2001) in Fig. 4. The further discussion is deferred to Sect. 5.

3.4. Correlations of the helium abundance with stellar parameters?

In order to search for possible trends of the chemical composition with the atmospheric parameters we compare the derived helium abundances with the measured stellar parameters $T_{\rm eff}$, log(g), and with the luminosity[2] for all apparently single EHB programme stars in Figs. 5–7.

First of all, we discovered a clear correlation between the helium abundance and the effective temperature ($T_{\rm eff}$): The larger the temperature, the larger the helium content (cf. Fig. 5). Furthermore, there seems to be a separation into two sequences of sdB stars in the $T_{\rm eff}$ – helium abundance plane. A fraction of our analysed sdB stars (about 1/6th, indicated with filled

[2] We express the luminosity in terms of the Eddington Luminosity $L_{\rm e}$ (for electron scattering, see Eq. (1)).

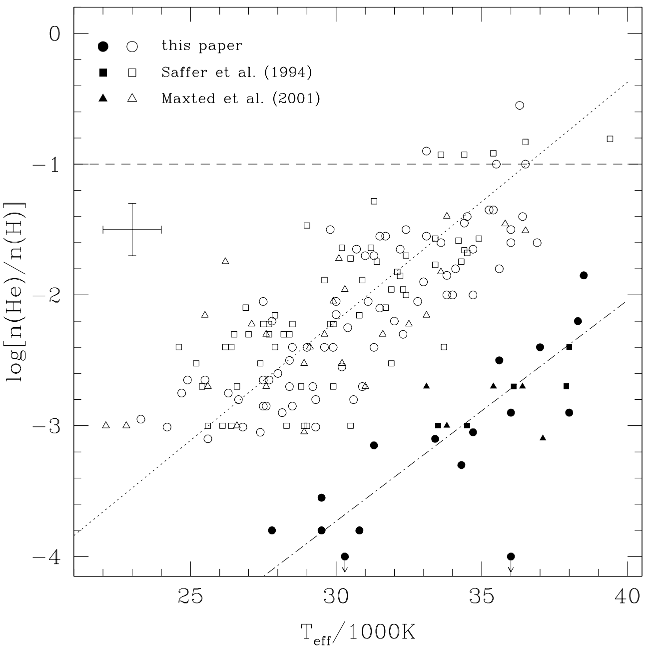

Fig. 5. Plot of the helium abundance versus effective temperature. Additionally the results of Saffer et al. (1994, squares) and Maxted et al. (2001, triangles) are plotted. The dotted line indicates the linear regression (Eq. (2)) for the bulk of the sdB stars (open symbols) and the dashed-dotted line shows the linear regression (Eq. (3)) for the peculiar sdB stars (filled symbols). The dashed horizontal line denotes the solar helium abundance.

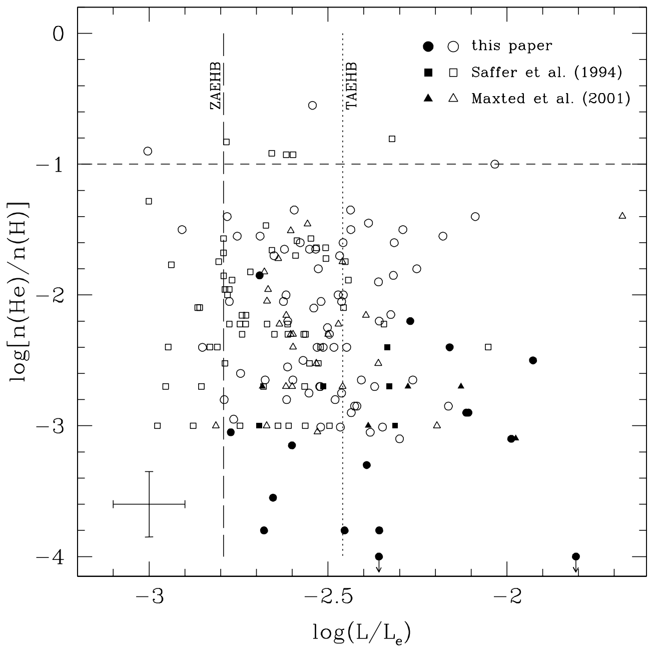

Fig. 7. Plot of the helium abundance versus luminosity (with respect to the Eddington luminosity L_e, see Eq. (1)). Additionally the results of Saffer et al. (1994, squares) and Maxted et al. (2001, triangles) are plotted. The dashed horizontal line denotes the solar helium abundance, the long dashed vertical line denotes the ZAEHB, and the dotted vertical line the TAEHB. For the filled symbols cf. Fig. 5.

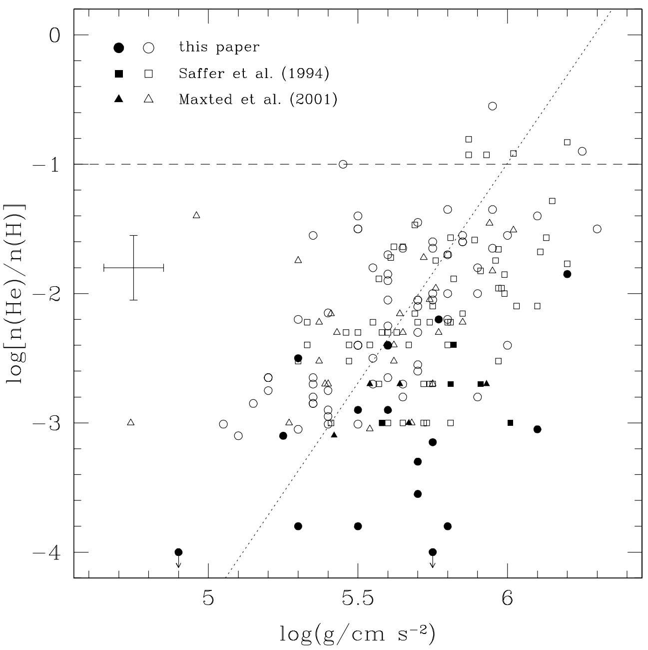

Fig. 6. Plot of the helium abundance versus gravity. Additionally the results of Saffer et al. (1994, squares) and Maxted et al. (2001, triangles) are plotted. The dashed horizontal line denotes the solar helium abundance. For the filled symbols cf. Fig. 5. The dotted line is the linear regression for the bulk of the sdB stars (open symbols).

symbols) have much lower helium abundances at the same temperatures than the bulk of the sdB stars.

Figure 6 may indicate a connection between the helium abundance and the gravity. However, for sdB stars the gravity is not independent of the effective temperature (see Eq. (1)) since the horizontal branch is a sequence of nearly constant luminosity. The stars that seperate from the main bulk (filled circles) in Fig. 5 lie somewhat below the main bulk in Fig. 6 as well, but do not separate as clearly as in the former diagram.

The luminosity as derived from gravity and $T_{\rm eff}$

$$L/L_{\rm e} = T_{\rm eff}^4/(10^{15.118} \times g) \tag{1}$$

is plotted in Fig. 7. No correlation is detectable. However, for the peculiar sdB stars (indicated with filled symbols) there is a slight tendency for a correlation to occur at higher luminosities.

To verify our discoveries, we have searched in the literature for other analyses which determined the atmospheric parameters using a method similar to ours. The results of Saffer et al. (1994, squares) who analysed 68 EHB stars and those of Maxted et al. (2001, triangles) who analysed 36 EHB stars for atmospheric parameters are added to ours in Figs. 5 to 7. The correlation between the helium abundance and the effective temperature is confirmed. Furthermore, the suggested separation into two sequences (cf. Fig. 5) is reinforced.

A linear regression for the bulk of sdB stars (open symbols) gives:

$$\log\left[\frac{n(\rm He)}{n(\rm H)}\right] = -3.53 + 1.35\left(\frac{T_{\rm eff}}{10^4\,\rm K} - 2.00\right). \tag{2}$$

For the other sequence (filled symbols, except the two upper limit values indicated by downward arrows) we get:

$$\log\left[\frac{n(\mathrm{He})}{n(\mathrm{H})}\right] = -4.79 + 1.26\left(\frac{T_{\mathrm{eff}}}{10^4\ \mathrm{K}} - 2.00\right). \quad (3)$$

3.5. Comparison with previous results

Spectroscopic analyses are available in the literature only for five of our programme stars from three different groups (Moehler et al. 1990a; Bixler et al. 1991; Saffer et al. 1994).

Different methods were applied to determine the stellar parameters: Two groups (Bixler et al. 1991; Saffer et al. 1994) used a procedure similar to the one described here (fitting of model line profiles to optical spectra) to derive T_{eff} and $\log(g)$. Saffer et al. included the determination of the helium abundance into their fit process, whereas Bixler et al. derived the helium abundance from equivalent width measurement of the He I 4471 Å, 4922 Å, and He II 4686 Å lines. Moehler et al. (1990a) used a three-step-procedure: The effective temperature has been calculated first from colour indices. Keeping the temperature fixed, the surface gravity was obtained by visual comparison of model line profiles with optical spectra of one or more Balmer lines (mainly H_γ). Finally, the helium abundance was derived by measuring the equivalent width of the He I 4471 Å line.

The sample of Bixler et al. (1991) overlaps with ours for three stars (HS 0039+4302, HS 1641+4601, and HS 2233+2332). However, the results given in Bixler et al. (1991) suffer from very large error limits ($\Delta T_{\mathrm{eff}}/T_{\mathrm{eff}} \approx$ 15–20%, $\Delta\log(g) \approx$ 0.4–0.7 dex) probably due to the low resolution and S/N of their spectra, which renders a comparison with our results useless.

One star (HS 0212+1446) overlaps with the sample of Moehler et al. (1990a). The values differ considerably: the effective temperature determined by Moehler et al. (1990a) is 5000 K lower and the gravity is 0.9 dex lower than our results. Saffer et al. (1994), who discovered similar differences comparing their results with that of Moehler et al. (1990a), argue that the calibration of the Strömgren colours used by Moehler et al. (1990a) is inappropriate for sdB stars and causes larger systematic errors. This view is supported by investigations of Napiwotzki et al. (1993).

There remains only one sdB star of our sample that can be compared with the results of another group. Saffer et al. (1994) determined the stellar parameters for HS 1236+4754 to be $T_{\mathrm{eff}} = 27\,900$ K $\pm$ 1000 K, $\log(g) = 5.47 \pm 0.15$, and $n(\mathrm{He})/n(\mathrm{H}) = 0.004$, which is in perfect agreement with our result: $T_{\mathrm{eff}} = 28\,400$ K $\pm$ 800 K, $\log(g) = 5.55 \pm 0.10$, and $n(\mathrm{He})/n(\mathrm{H}) = 0.003$.

4. Radial velocities and distances

4.1. Radial velocities

In view of the large fraction of single lined binaries among the sdB stars (Maxted et al. 2001) it is worthwhile to measure radial velocities (RVs) of our programme stars. The RVs are determined by calculating the shifts of the measured wavelengths of all fitted Balmer and helium lines relative to laboratory wavelengths. Afterwards they are corrected to heliocentric values. We decided to determine the RVs only for spectra with spectral resolutions equal to or better than 3.6 Å, because the error margins for the spectra of lower resolution are too large to yield meaningful results.

The resulting values are accurate to about ± 30 km s^{-1} and can be found in Table 4. Out of four stars which were observed twice at different dates, only one (HS 2333+3927) is found to be a RV variable. The resulting velocities for the other sdB stars, which are observed only once, are given in Table 4 for comparison with future RV measurements.

4.2. Distances

We calculated the distances for all sdB programme stars, assuming a canonical mass of 0.5 $M_\odot$. From the derived gravities, the radii of the stars are calculated. By comparing the model atmosphere flux with the dereddened apparent visual magnitude[3], the angular diameter of a star could be determined. Because several of the programme stars lie at relatively low galactic latitudes ($20° < |b_{\mathrm{II}}| < 30°$), interstellar reddening can be significant, e.g. as high as $E(B-V) = 0\overset{\mathrm{m}}{.}3$ for HS 0357+0133 (see Table 4). All stars lie at distances between 300pc and several kiloparsec from the galactic plane, therefore beyond the galactic dust layer. The reddening for all programme stars are estimated from the maps of Schlegel et al. (1998). From radii and angular diameters, the distances of the stars follow immediately. The distance z from the galactic plane is derived from the galactic latitudes: $z = d \times \sin(b_{\mathrm{II}})$. The results are listed in Table 4.

Three programme stars are apparently normal B stars. Assuming that they are main sequence stars, we derive masses for HS 0231+8019, HS 1556+6032, and HS 2131+0349 of 5.5 $M_\odot$, 4.2 $M_\odot$, and 5.0 $M_\odot$, respectively, using the procedure of Ramspeck et al. (2001). Using these masses we get distances d (and $|z|$) of $\approx$21 kpc (7 kpc) for HS 0231+8019, $\approx$21 kpc (11 kpc) for HS 2131+0349, and $\approx$27 kpc (19 kpc) for HS 1556+6032. The z distances determined for HS 0231+8019 and HS 2131+0349 are not extraordinary in comparison to other known apparently normal B stars at high latitudes which are closer than about 10 kpc from the galactic plane (Rolleston et al. 1999; Ramspeck et al. 2001). However, HS 1556+6032 seems to be clearly farther away than other known apparently normal B stars in the halo of our Milky Way.

5. Discussion

In the gravity versus effective temperature plane (Fig. 3), our confirmed sdB and sdOB stars lie in a region close to the EHB, but with a tendency to cluster near the TAEHB when the He-core burning diminishes and the phase of helium shell burning starts. However, according to the evolutionary life times, most

[3] The visual magnitudes are estimated from the B magnitudes by adding the typical intrinsic colour of $B - V = -0.28$ mag (Altmann et al. in prep.).

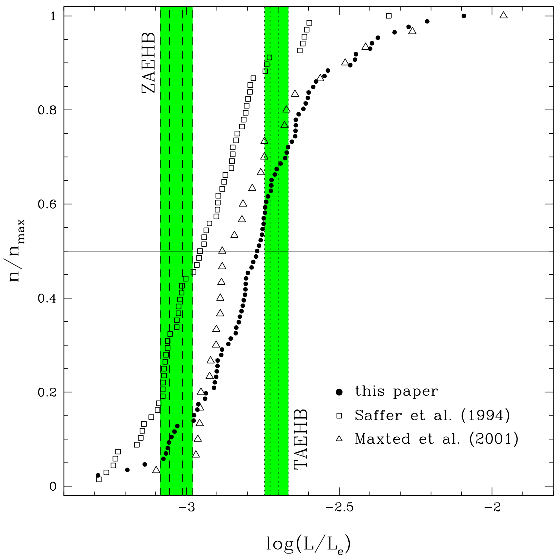

Fig. 8. Plot of (normalized) numbers of stars versus luminosity (with respect to the Eddington luminosity L_e, see Eq. (1)). Additionally are plotted the results of Saffer et al. (1994, open squares) and Maxted et al. (2001, open triangles). The dashed vertical lines denote the ZAEHB, and the dotted vertical lines the TAEHB for metallicities of [M/H] = 0.00, −0.47, −1.48, and −2.22, respectively from the left to the right (Dorman et al. 1993).

stars should be found closer to the ZAEHB, like seen in Heber (1986, Fig. 6), Saffer et al. (1994, Fig. 5), and Maxted et al. (2001, Fig. 2). Comparing our results (Fig. 3) to that of Saffer et al. (1994) and/or Maxted et al. (2001) (see Fig. 4), a systematic difference can be suggested. Saffer et al. (1994) even found some sdB stars (mostly at low temperature, $T_{\rm eff}$ = 25 000 to 27 000 K) to lie below the ZAEHB (cf. Fig. 4). Because only one star is common to in both studies (both sets of parameters agreed very well, see Sect. 3.4), a direct comparison was possible for this case only. We can, however, compare the samples in a global sense using the cumulative luminosity functions. In Fig. 8 we plot these functions for our sample and those of Saffer et al. (1994) and Maxted et al. (2001). The luminosity is expressed in units of the Eddington luminosity (Eq. (1)). Additionally the positions of the ZAEHB and the TAEHB are indicated. Since the metallicity of the stars is unknown, we have plotted models for various metallicity ranging from [M/H] = −2.22 to 0.00 (Dorman et al. 1993). Note that the position of the TAEHB is model-dependent, because poorly understood processes such as semiconvection and convective instabilities (breathing pulses, Castellani et al. 1985) play a role. As can be seen from Fig. 8, the overall shape of the cumulative luminosity function is similar for all three samples when the considerable smaller number of stars in the Maxted et al. (2001) sample is taken into account. However, there is an offset of about 0.2 dex in luminosity between the Saffer et al. (1994) sample and ours, whereas the relation for the Maxted et al. (2001) sample is in better agreement with ours. Possible reasons for the discrepancy are different observations, the different synthetic spectra used in the analysis, or both. Maxted et al. (2001) and our study is based on the same grid of NLTE models for stars hotter than 27 000 K and metal line blanketed LTE models for the cooler ones, whereas Saffer et al. (1994) use metal-free LTE models for all stars. The observations of Maxted et al. (2001) are of considerably higher spectral resolution than that of Saffer et al. (1994) and ours and on average have a better S/N than our data. The wavelength coverage of the observations also varies. Differences in synthetic spectra calculated from different sets of model atmospheres have already been reported. Heber et al. (2000) studied the influence of NLTE effects versus metal line blanketing in LTE and found that NLTE models give luminosities larger by about 0.1 dex than metal line blanketed LTE models. Therefore about half of the observed offset between the cumulative luminosity functions of Saffer et al. (1994) and ours can be traced back to NLTE effects, but an 0.1 dex offset remains unexplained. We have embarked on a more detailed investigation of this problem. It will be presented in a forthcoming paper.

Our analysis reveals an apparent correlation between the photospheric helium content and the stellar parameters of a sdB star: The larger the effective temperature and/or gravity, the larger the helium abundance. However, for sdB stars, $T_{\rm eff}$ and gravity are strongly connected and a plot of helium abundance versus luminosity does not reveal any correlations. There is general consensus that the low helium abundance of sdB stars is due to diffusion processes. Simple diffusion models assume the abundances to be set by the equilibrium of gravitational and radiative forces. Such models predict helium abundances far lower than observed (Fontaine & Chayer 1997). Weak radiation-driven stellar winds, however, are likely to be present. Calculations by Fontaine & Chayer (1997) and Unglaub & Bues (2001) indeed show that a better agreement of the predicted helium abundance with observations can be achived by considering mass loss rates of the order of 10^{-14}–10^{-12} $M_\odot$/year. Radiation-driven wind theory predicts mass loss rates to increase with luminosity (Pauldrach et al. 1988). However, no such trend becomes apparent on our observations. Therefore, we conclude that other physical processes must be considered.

Additionally, a population of stars with very low helium abundances was identified when the helium abundance is plotted versus the effective temperature. These stars clearly separate from the bulk (see Fig. 5). The separation of these stars is much less evident when we plot the helium abundance versus the gravity (Fig. 6) or the luminosity (Fig. 7). This phenomenon provides evidence that surface abundances of sdB stars are not a simple function of their position in the HR diagram. It rules out time-independent diffusion models and points to a dependence on the star's history. Due to the discovery of Maxted et al. (2001), that about 2/3rd of all sdB stars appear to be RV variable, it is very likely that many sdB stars in our sample are members of a close binary system with an unseen companion, like HS 2333+3927 already discovered. Aznar Cuadrado & Jeffery (2002) suggest that short-period binaries may have a larger photospheric helium content than long-period binaries due to tidal effects disturbing the diffusive separation inside sdB stars (see above) in short-period systems more than in long-period systems. Therefore, the separation into two sequences of helium abundances possibly could be caused by their (yet undetected) binary nature.

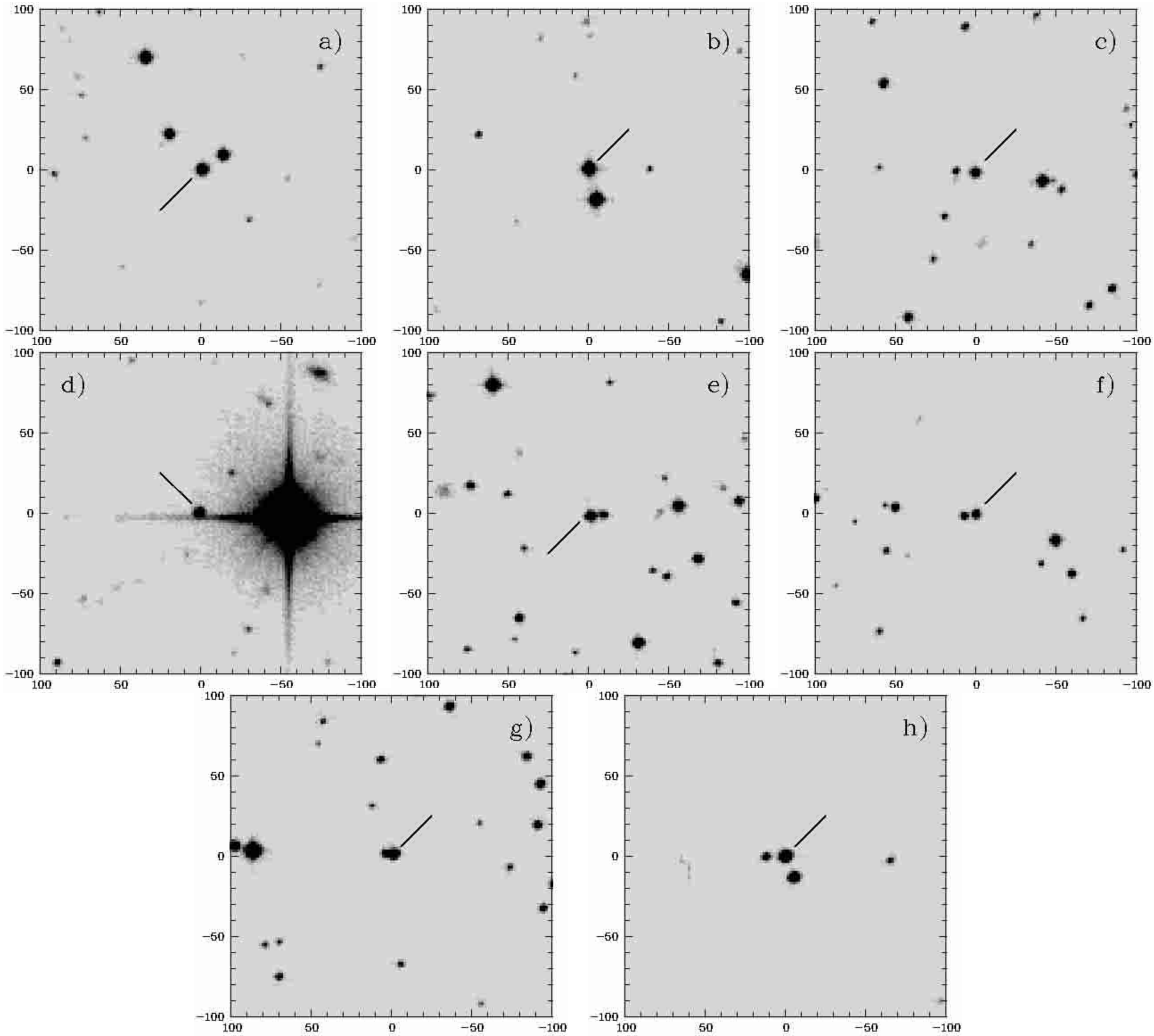

Fig. 9. HQS finding charts of selected subdwarfs: **a)** HS 0039+4302, **b)** HS 0213+2329, **c)** HS 0600+6602, **d)** HS 1320+2622, **e)** HS 2100+1710, **f)** HS 2143+8157, **g)** HS 2206+2847, **h)** HS 2229+0910. The charts are centered on the coordinates given in Table 4 and the size is 200″ × 200″. East is left and North is up.

6. Conclusions

We have presented the results of a spectral analysis of 111 sdB candidates selected from follow-up observations of the Hamburg Quasar Survey. The analysis reveals 89 stars to be bona fide subdwarf B and subdwarf OB stars. The remaining objects are 18 spectroscopic binaries containing a sdB component, one HBB, and three apparently normal B stars. Stellar parameters as well as radial velocities and distances have been determined. The results are largely consistent with the results from the literature by other groups, when NLTE effects are accounted for. To resolve the reason for the remaining differences, however, a detailed investigation of systematic errors caused by different observational material and by the use of different model atmospheres is required.

Additionally, there remain two open questions: What physical processes cause the discovered correlation of the helium abundance with the effective temperature? Why is there a separation into two sequences of sdB stars in the $T_{\rm eff}$–helium abundance plane? To understand these phenomena, more observations and further calculations are urgently needed.

Last but not least, our spectral analysis was also the starting point of another investigation: The majority of our programme stars lie in a temperature range where non-radial pulsations have been predicted to occur (Charpinet et al. 1996) and have indeed been observed (Kilkenny et al. 1997). Therefore we initiated a collaboration with two groups in Norway and Italy in 1999 to search for pulsating sdB stars in our sample. All of our stars will be observed for light variations. Up to June 2002, about 70 HQS sdB stars had been observed and nine (HS 0039+4302, HS 0444+0408, HS 0702+6043, HS 0815+4243, HS 1824+5745, HS 2149+0847, HS 2151+0857, HS 2201+2610, and HS 2303+0152) were found to be pulsating (Østensen et al. 2000a,b;

Dreizler et al. 2002; Silvotti et al. 2002). This represents about one pulsator in ten sdB stars. It also means that about one third of all known sdBV stars discovered so far have been drawn from our investigation presented here. The photometric monitoring also led to the discovery of a short period eclipsing binary of the HW Vir type (HS 0705+6700, Drechsel et al. 2001) which is only the third member of this class.

Acknowledgements. Thanks go to all those colleagues who participated in the observing campaigns: S. Jordan, R. Möller, H. Marten, S. Haas, and also to the staff of the Calar Alto observatory, Spain, for their valuable assistance during our visits. Additionally we are grateful to T. Rauch for providing us with his spectrum. We thank Dr. C. S. Jeffery, the referee, for his valuable suggestions which helped to improve the paper. H.E. acknowledges financial support by the German research foundation DFG under grant He 1354/30−1 and for several travel grants to the Calar Alto observatory. The HQS was supported by DFG grants Re 353/11 and Re 353/22. This research has made use of the SIMBAD database, operated at CDS, Strasbourg, France.

References

Abrahamian, H. V., Lipovetsky, V. A., Mickaelian, A. M., & Stepanian, D. A. 1990, Afz, 33, 345
Abrahamian, H. V., & Mickaelian, A. M. 1996, Astrophysics, 39, 315
Allard, F., Wesemael, F., Fontaine, G., Bergeron, P., & Lamontagne, R. 1994, AJ, 107, 1565
Aznar Cuadrado, R., & Jeffery, C. S. 2002, A&A, 385, 131
Barnard, A. J., Cooper, J., & Smith, E. W. 1974, JQSRT, 14, 1025
Baschek, B., & Norris, J. 1975, ApJ, 199, 694
Berger, J., & Fringant, A. M. 1977, A&AS, 28, 123
Bergeron, P., Saffer, R. A., & Liebert, J. 1992, ApJ, 394, 228
Bixler, J. V., Bowyer, S., & Laget, M. 1991, A&A, 250, 370
Brown, T. M., Ferguson, H. C., Davidsen, A. F., & Dorman, B. 1997, ApJ, 482, 685
Brown, T. M., Bowers, C. W., & Kimble, R. A. 2000a, ApJ, 529, L89
Brown, T. M., Bowers, C. W., Kimble, R. A., Sweigart, A. V., & Ferguson, H. C. 2000b, ApJ, 532, 308
Castellani, V., Chieffi, A., Tornambe, A., & Pulone, L. 1985, ApJ, 296, 204
Charpinet, S., Fontaine, G., Brassard, P., & Dorman, B. 1996, ApJ, 471, L103
Charpinet, S., Fontaine, G., Brassard, P., et al. 1997, ApJ, 483, L123
Charpinet, S. 2001, Astron. Nachr., 322, 387
Dorman, B., Rood, R. T., & O'Connell, R. W. 1993, ApJ, 419, 596
Drechsel, H., Heber, U., Napiwotzki, R., et al. 2001, A&A, 379, 893
Dreizler, S., Heber, U., Werner, K., Moehler, S., & de Boer, K. S. 1990, A&A, 235, 234
Dreizler, S., Heber, U., Jordan, S., & Engels, D. 1994, Proc. of the IAU Colloq., 180, ed. S. J. Adelman, A. R. Upgren, & C. J. Adelman (Cambridge Univ. Press), Hot stars in the Galactic Halo, 228
Dreizler, S., Schuh, S., Deetjen, J. L., Edelmann, H., & Heber, U. 2002, A&A, 386, 249
Fontaine, G., & Chayer, P. 1997, Conf. on Faint Blue Stars, ed. A. G. D. Philip, J. Liebert, R. Saffer, & D. S. Hayes (L. Davis Press), 169
Green, E. M., Liebert, J., & Saffer, R. A. 2001,
Green, R. F., Schmidt, M., & Liebert, J. 1986, ApJS, 61, 305, Proc. of the 12th European Workshop on White Dwarfs, ed. J. L. Provencal, H. L. Shipman, J. MacDonald, & S. Goodchild, ASP Conf. Ser., 226, 192
Griem, H. R. 1974, Spectral line broadening by plasmas, Pure and Applied Physics (New York: Academic Press)
Hagen, H.-J., Groote, D., Engels, D., & Reimers, D. 1995, A&AS, 111, 195
Hagen, H.-J., Engels, D., & Reimers, D. 1999, A&AS, 134, 483
Haro, G., & Luyten, W. J. 1962, Bol. Inst. Tonantzintla 3, 37
Heber, U., Hunger, K., Jonas, G., & Kudritzki, R. P. 1984, A&A, 130, 119
Heber, U. 1986, A&A, 155, 33
Heber, U., Jordan, S., & Weidemann, V. 1989, Proc. of the Astron. Gesellschaft, Abstract Ser., 3, 94
Heber, U., Jordan, S., & Weidemann, V. 1991, Proc. of the 7th European Workshop on White Dwarfs, ed. G. Vauclair, & E. Sion., NATO Advanced Science Institutes (ASI) Ser. C, 336, 109
Heber, U., Dreizler, S., & Hagen, H.-J. 1996, A&A, 311, L17
Heber, U., Reid, I. N., & Werner, K. 2000, A&A, 363, 198
Homeier, D., Koester, D., Hagen, H.-J., et al. 1998, A&A, 338, 563
Homeier, D., Koester, D., Jordan, S., et al. 1999, Proc. of the 11th European Workshop on White Dwarfs, ed. J.-E. Solheim, & E. G. Meištas, ASP Conf. Ser., 169, 37
Humason, M. L., & Zwicky, F. 1947, ApJ, 105, 85
Iriarte, B., & Chavira, E. 1957, Bol. Obs. Tonantz. Tacub., 2, part No. 16, 3
Kilkenny, D. 1984, MNRAS, 211, 969
Kilkenny, D., Koen, C., O'Donoghue, D., & Stobie, R. S. 1997, MNRAS, 285, 640
Kurucz, R. L. 1979, ApJS, 40, 1
Lemke, M., Heber, U., Napiwotzki, R., Dreizler, S., & Engels, D. 1997a, Proc. of the 3rd Conf. on Faint Blue Stars, ed. A. G. D. Philip, J. Liebert, R. Saffer, & D. S. Hayes (L. Davis Press), 375
Lemke, M. 1997b, A&AS, 122, 285
Markarian, B. E., & Stepanian, J. A. 1983, Afz, 19, 639
Maxted, P. F. L., Marsh, T. R., & North, R. C. 2000, MNRAS, 317, L41
Maxted, P. F. L., Heber, U., Marsh, T. R., & North, R. C. 2001, MNRAS, 326, 1391
Mengel, J. G., Norris, J., & Gross, P. G. 1976, ApJ, 204, 488
Mitchell, K. J. 1998, ApJ, 494, 256
Moehler, S., de Boer, K. S., & Heber, U. 1990a, A&A, 239, 265
Moehler, S., Richtler, T., de Boer, K. S., Dettmar, R. J., & Heber, U. 1990b, A&AS, 86, 53
Napiwotzki, R., Schönberner, D., & Wenske, V. 1993, A&A, 268, 653
Napiwotzki, R. 1997, A&A, 322, 256
Noguchi, T., Maehara, H., & Kondo, M. 1980, Tokyo, University, Tokyo Astronomical Observatory, Annals, Second Ser., vol. 18, No. 1, 55
O'Donoghue, D., Koen, C., Kilkenny, D., & Stobie, R. S. 1999, Proc. of the 11th European Workshop on White Dwarfs, ed. J.-E. Solheim, & E. G. Meištas, ASP Conf. Ser., 169, 149
Oke, J. B. 1990 AJ, 99, 1621
Østensen, R., Solheim, J.-E., Heber, U., et al. 2001a, A&A, 368, 175
Østensen, R., Heber, U., Silvotti, R., et al. 2001b, A&A, 378, 466
Paczyński, B. 1971, Acta Astron., 21, 1
Pesch, P., & Sanduleak, N. 1983, ApJS, 51, 171
Pauldrach, A., Puls, J., Kudritzki, R. P., Mendez, R. H., & Heap, S. R. 1988, A&A, 207, 123
Pickering, E. C., & Kapteyn, J. C. 1918, Ann. Astron. Obs. Harvard Coll., 101
Ramspeck, M., Heber, U., & Moehler, S. 2001, A&A, 378, 907
Rodgers, A. W., Roberts, W. H., & Walker, I. 1993, AJ, 106, 591
Rolleston, W. R. J., Hambly, N. C., Keenan, F. P., Dufton, P. L., & Saffer, R. A. 1999, A&A, 347, 69
Saffer, R. A., Bergeron, P., Koester, D., & Liebert, J. 1994, ApJ, 432, 351
Saffer, R. A., Livio, M., & Yungelson, L. R. 1998, ApJ, 502, 394

Schlegel, D. J., Finkbeiner, D. P., & Davis, M. 1998, ApJ, 500, 525
Schöning, T., & Butler, K. 1989, A&AS, 78, 51
Shamey Louis, J. 1969, Ph.D. Thesis, Loyola University of Los Angeles
Silvotti, R., Østensen, R., Heber, U., et al. 2002, A&A, 383, 239
Theissen, A., Moehler, S., Heber, U., & de Boer, K. S. 1993, A&A, 273, 524
Theissen, A., Moehler, S., Heber, U., Schmidt, J. H. K., & de Boer, K. S. 1995, A&A, 298, 577
Thejll, P., Theissen, A., & Jimenez, R. 1994, A&A, 292, 457
Tüg, H. 1977, ESO Messenger, 11, 7
Unglaub, K., & Bues, I. 2001, A&A, 374, 570
Usher, P. D. 1981, ApJS, 46, 117
Vidal, C. R., Cooper, J., & Smith, E. W. 1973, ApJS, 25, 37
Wegner, G., & Swanson, S. R. 1990, AJ, 100, 1274
Werner, K., & Husfeld, D. 1985, A&A, 148, 417
Werner, K. 1986, A&A, 161, 177